ACES Asian Chemical Editorial Society

doi.org/10.1002/asia.202401419

CHEMISTRY AN ASIAN JOURNAL Research Article

www.chemasianj.org

Efficient Capture of ReO_4^- from Water by Imidazolium-Based Cationic Polymeric Nanotraps

Xiaorui Li[+],[a, c] Wenping Liu[+],[b] Haiying Wang,[c] Yingjie He,[c] Wei Liu,[b] Huan Li,[a] Linfeng Jin,[a] Changqing Su,[a] Yiming Li,*[b] Thamraa AlShahrani,[e] and Shengqian Ma*[d]

Rhenium represents an irreplaceable metal resource, which finds extensive applications in diverse fields, particularly in the aerospace and petrochemical industry. However, its remarkably low natural abundance and the lack of independent ore deposits pose significant challenges to its extraction and recovery processes. In this study, we present the highly efficient adsorption of perrhenate by a cationic polymeric nanotrap material, namely CPN-3VIm. The maximum adsorption capacity of CPN-3VIm-Cl for ReO_4^- attains an impressive value of 1220 $mg \cdot g^{-1}$. Notably, even in the low-concentration ReO_4^- solution of 8.5 ppm, the removal rate could still exceed 99%. The recycling performance of CPN-3VIm-Cl also shows exceptional results, with both ReO_4^- removal and recovery rates surpassing 90% throughout five adsorption-desorption cycles. Furthermore, CPN-3VIm-Cl exhibits nearly 100% extraction efficiency for ReO_4^- within a broad pH range of 4–10 and demonstrates remarkable structural stability under extreme conditions, such as 3 M sulfuric acid or 3 M nitric acid. Additionally, a comprehensive investigation into the interaction mechanism between CPN-3VIm-Cl and perrhenate was carried out using SEM-EDS mapping, Raman, FT-IR, and XPS analysis.

Introduction

Rhenium constitutes an essential and irreplaceable metal resource, which has been widely exploited in pivotal fields such as aerospace and petrochemical industry.[1] In the aerospace industry, it plays a crucial role in manufacturing high-temperature components of jet engines, owing to its outstanding resistance to heat and corrosion. While in the petrochemical sector, it is utilized in catalysts for complex chemical reactions, enhancing the efficiency and productivity of various processes. Nonetheless, its exceedingly scarce abundance and the dearth of independent ore deposits have substantially constrained its extraction procedures and subsequent applications. The terrestrial crust exhibits a rhenium abundance merely on the scale of 10^{-9}, making it one of the rarest elements on Earth.[2] Furthermore, rhenium is customarily affiliated with copper or molybdenum deposits, leading to its extraction predominantly occurring as a byproduct from the wastewater generated during copper or molybdenum smelting operations.[3] Presently, within the context of copper smelting procedures, rhenium predominantly assumes the form of perrhenate(ReO_4^-) in acidic wastewater.[1b] However, the harsh conditions of smelting wastewater, including potent acidity, extremely low rhenium concentration, as well as a copious quantity of competing anions, render the extraction and recovery of rhenium exceptionally arduous.[3–4] The pronounced acidity makes the majority of adsorbent materials unstable, thereby leading to a deterioration in their recycling performance. Moreover, the extremely low concentration of perrhenate anions and the substantial presence of competing ions conspire results in extremely low adsorption efficiency for most non-selective adsorbent materials.

To address the challenge of selective perrhenate extraction, researchers have fabricated a diverse array of adsorption materials,[5] encompassing MOFs,[6] COFs, inorganic composites,[7] and so on.[8] Among them, cationic polymers, as an emerging class of adsorption material, have achieved significant advancements in the research domain of perrhenate extraction.[9] This novel material features fixed cationic moieties on the polymer backbone, such as pyridinium salts,[10] imidazolium salts,[11] quaternary ammonium salts,[12] etc.[13] The adsorption mechanism is actualized through ion exchange between the material's free counterions and the anions present in aqueous solutions.[14] By means of modifying or substituting the cationic functional groups, a multitude of designable attributes can be attained, including high absorption capacity, notable perrhenate selectivity, and rapid kinetic process.[15] However, given the complexity of industrial rhenium-containing waste-

[a] X. Li,[+] H. Li, L. Jin, C. Su
School of Resource & Environment, Hunan Provincial Key Laboratory of Carbon Neutrality and Intelligent Energy, Hunan University of Technology and Business, Changsha, Hunan, 410205, China

[b] W. Liu,[+] Prof. W. Liu, Prof. Y. Li
College of Chemistry and Chemical Engineering, Central South University, Changsha, Hunan, 410083, China
E-mail: chemyl@csu.edu.cn

[c] X. Li,[+] Prof. H. Wang, Y. He
School of Metallurgy and Environment, Central South University, Changsha, Hunan, 410083, China

[d] Prof. S. Ma
Department of Chemistry, University of North Texas, Denton, TX, 76201, USA
E-mail: Shengqian.Ma@unt.edu

[e] T. AlShahrani
Department of Physics, College of Science, Princess Nourah bint Abdulrahman University, Riyadh 11564, Saudi Arabia

[+] These authors contributed equally to this work.

Supporting information for this article is available on the WWW under https://doi.org/10.1002/asia.202401419

water, it is of paramount importance to develop a material that can strike a balance between capture capacity, deep uptake, and a wide pH adaptability for comprehensive rhenium recovery.[16]

Herein, we report a cationic polymeric nanotrap material, designated as CPN-3VIm (3VIm for three Vinyl Imidazolium arms), and the comprehensive investigation of its perrhenate adsorption performance in aqueous solution. Such material exhibited high adsorption capacity, profound extraction efficiency, and wide pH work range. Specifically, the maximum adsorption capacity of CPN-3VIm-Cl (CPN-3VIm with Cl^- as counterions) for ReO_4^- could attain up to 1220 $mg \cdot g^{-1}$, with a removal rate surpassing 99% even in a low-concentration ReO_4^- solution of 8.5 ppm. In addition, CPN-3VIm-Cl exhibited remarkable stability and a wide working pH range, enabling it to maintain a stable structure under strong acidic conditions, and to achieve an extraction rate proximate to 100% within the pH range of 4–10. Moreover, after the fifth cycle of adsorption-desorption process, the extraction and recovery rate of perrhenate could still reach as high as 98.7% and 98.5%, respectively. These exceptional properties not only confer CPN-3VIm-Cl with a highly promising application prospect in rhenium resource recovery, but also offer valuable guidelines for the design and application of cationic polymers.

Results and Discussion

Synthesis and Characterization of CPN-3VIm-Cl

CPN-3VIm-Br (CPN-3VIm with Br^- as counterions) was synthesized via a free radical polymerization reaction, employing the cationic unit 3VIm installed with three vinyl groups (Scheme 1, detailed synthetic route can be found in the Supporting Information). Subsequently, to improve the adsorption kinetic and the capacity, an ion exchange process from Br^- to Cl^- was carried out.[14,17] This was achieved by soaking CPN-3VIm-Br in a 2 M NaCl aqueous solution for three successive times, ultimately yielding CPN-3VIm-Cl.

To ascertain the structure of CPN-3VIm-Cl, solid-state ^{13}C NMR was initially employed. By making a comparison with the ^{13}C NMR spectrum of the precursor 3VIm, which served as a crucial reference,[18] the spectrum signal of CPN-3VIm-Cl could be comprehensively assigned. As depicted in Figure 1a, the signal peak at 130.67 ppm was ascribed to the C2 carbon atom of the benzene ring and C4 of the imidazole ring. The signal peak at 119.55 ppm was assigned to the C1 carbon of the benzene ring and C5 and C6 of the imidazole ring. Owing to the 2/1 integral area ratio of the peaks at 47.88 ppm and 35.81 ppm, the former peak was designated to carbon C3 and C7, and the latter peak was attributed to carbon C8.

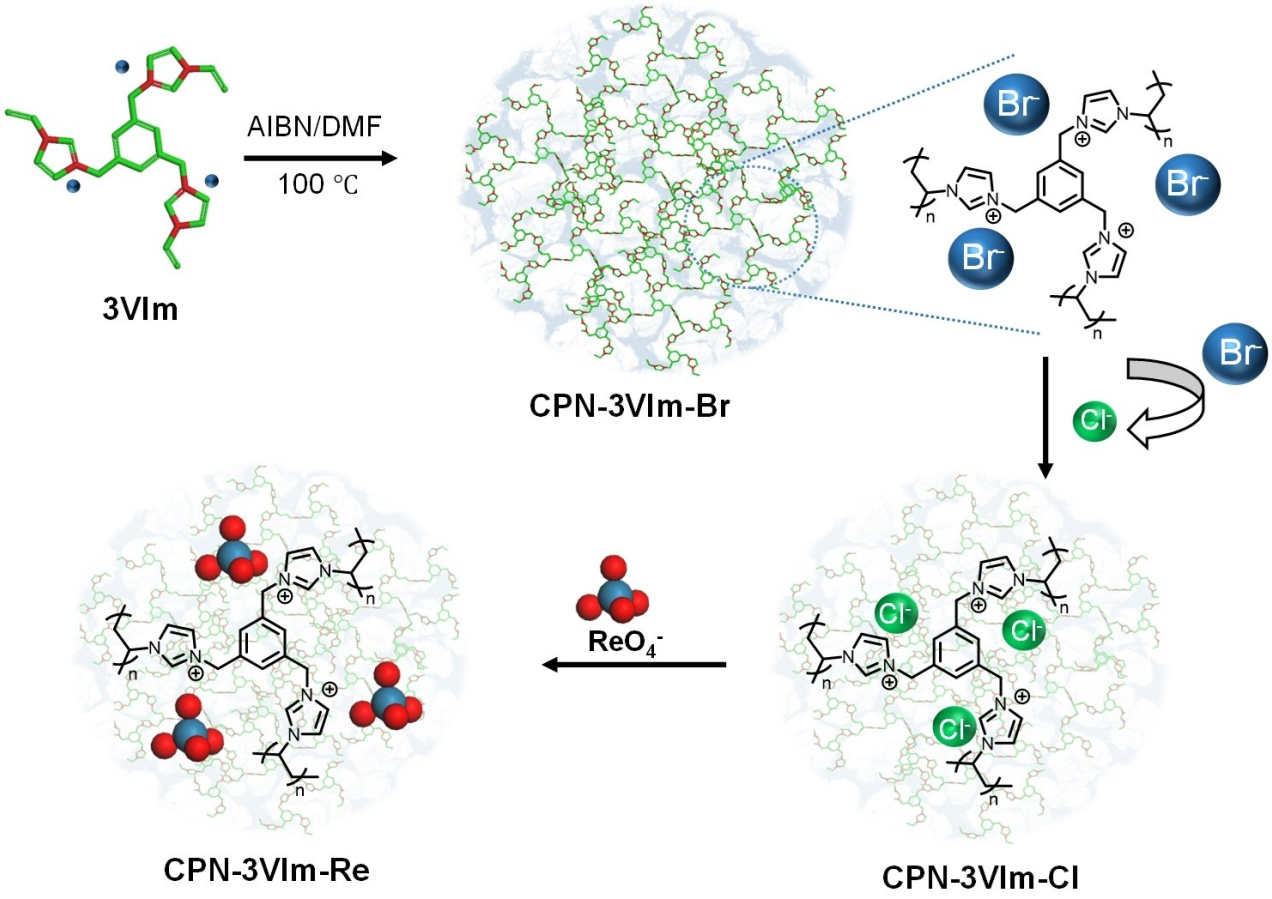

Scheme 1. Synthetic route of CPN-3VIm-Cl and the anion-exchange process.

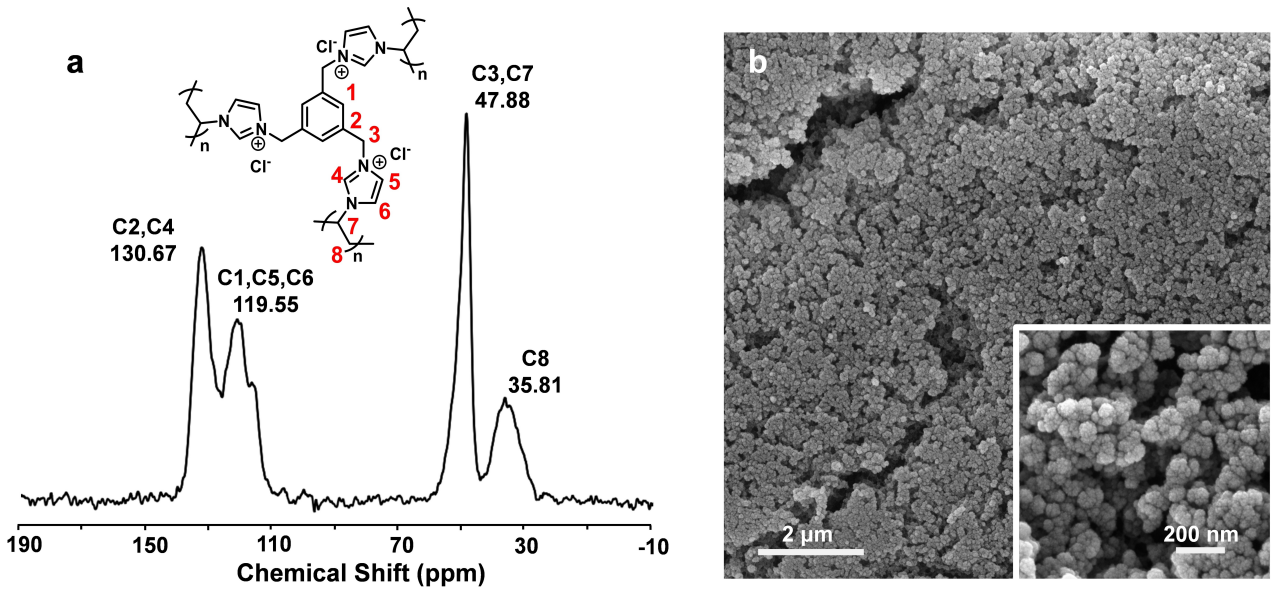

Figure 1. a) Solid-state ^{13}C NMR spectrum of CPN-3VIm-Cl. b) SEM image of CPN-3VIm-Cl.

Furthermore, Fourier transform infrared spectrometer (FT-IR) was utilized to identify the anticipated functional groups within the structure (Figure 4c). The broad peak spanning the range of 2900–3200 cm^{-1} could be attributed to the stretching vibrations of the C–H bonds on the imidazolium group and phenyl ring. The characteristic peaks of the imidazolium salt were detected at 1631 cm^{-1} and 1550 cm^{-1}, with the peak in the fingerprint region at 1150 cm^{-1} corresponding to the stretching vibration of the imidazolium salt skeleton.[19]

Subsequently, a suite of advanced technologies, including Scanning electron microscopy (SEM), Powder X-ray Diffraction (PXRD), were employed to probe the morphology of CPN-3VIm-Cl. Macroscopically, this cationic polymer manifested as an off-white powder (Figure S1, Supporting Information), while it exhibited a cauliflower-like morphology at the nanoscale (Figure 1b and Figure S5). The PXRD pattern of CPN-3VIm-Cl displayed a broad peak around 25° (Figure S2), indicating an amorphous nature of the material. Intriguingly, CPN-3VIm-Cl demonstrated a remarkable water vapor uptake capacity, reaching a maximum value up to 227 $cm^3 \cdot g^{-1}$ when the P/P_0 ratio reached 0.71 (Figure S3b). When P/P_0 was less than 1, a steep rise in the curve was evident, signifying the potent interaction between the positively charged polymer skeleton and water molecules. In contrast, no nitrogen adsorption behavior was detected for CPN-3VIm-Cl (Figure S3a), which could potentially be attributed to the ultra-microporous network that precluded N_2 entry.

Furthermore, comprehensive stability tests were conducted on CPN-3VIm-Cl. Thermogravimetric analysis (TGA) revealed an initial weight loss of approximately 16% at temperature 160 °C, which was mainly due to the evaporation of water (Figure S4). Remarkably, the material maintained its structural integrity up to 260 °C, attesting to its outstanding thermal stability. To further investigate the stability of the cationic polymer in acidic milieus, CPN-3VIm was immersed in 3M H_2SO_4 and 3M HNO_3 overnight to evaluate its applicability under extreme industrial conditions (Figure S6 and S7). The SEM images revealed that the morphology of post-soaking polymer remained nearly unchanged, further corroborating the excellent acid resistance of CPN-3VIm-Cl.

Sorption Investigation

Upon the completion of comprehensive characterization analyses to confirm the structure of CPN-3VIm-Cl, an in-depth investigation into its ReO_4^- uptake performance was carried out. The adsorption thermodynamics behavior was meticulously evaluated by means of adsorption isotherms of CPN-3VIm-Cl (Figure 2a, with an initial ReO_4^- concentration range from 10 to 1000 ppm). The experimental data was fitted using both the Langmuir isotherm model (inset in Figure 2a) and the Freundlich isotherm model (Figure S8). Notably, the Langmuir model exhibited superior performance, as evidenced by its higher correlation coefficient ($R^2 > 0.99$, the corresponding data was presented in Table S1). The maximum experimental adsorption capacity of 1220 $mg \cdot g^{-1}$ (as shown in Table S3) was marginally lower than the theoretical maximum sorption capacity (1493 $mg \cdot g^{-1}$, based on the theoretical sorption sites), under the presumption of a complete ion exchange process. Although it was slightly inferior to the current world record,[20] this data still ranked among the top tier of comparable material presently available.[21] A remarkable ReO_4^- removal percentage exceeding 99.5% was achieved when the initial concentration and the equilibrium concentration of the residual Re in the solution were 8.5 ppm and 39.9 ppb, respectively (Table S4). The results unequivocally demonstrated the excellent adsorption performance of CPN-3VIm-Cl towards ReO_4^-, which could be ascribed to the efficient ion exchange process between ReO_4^- and counter anions (Cl^-) on the cationic skeleton.

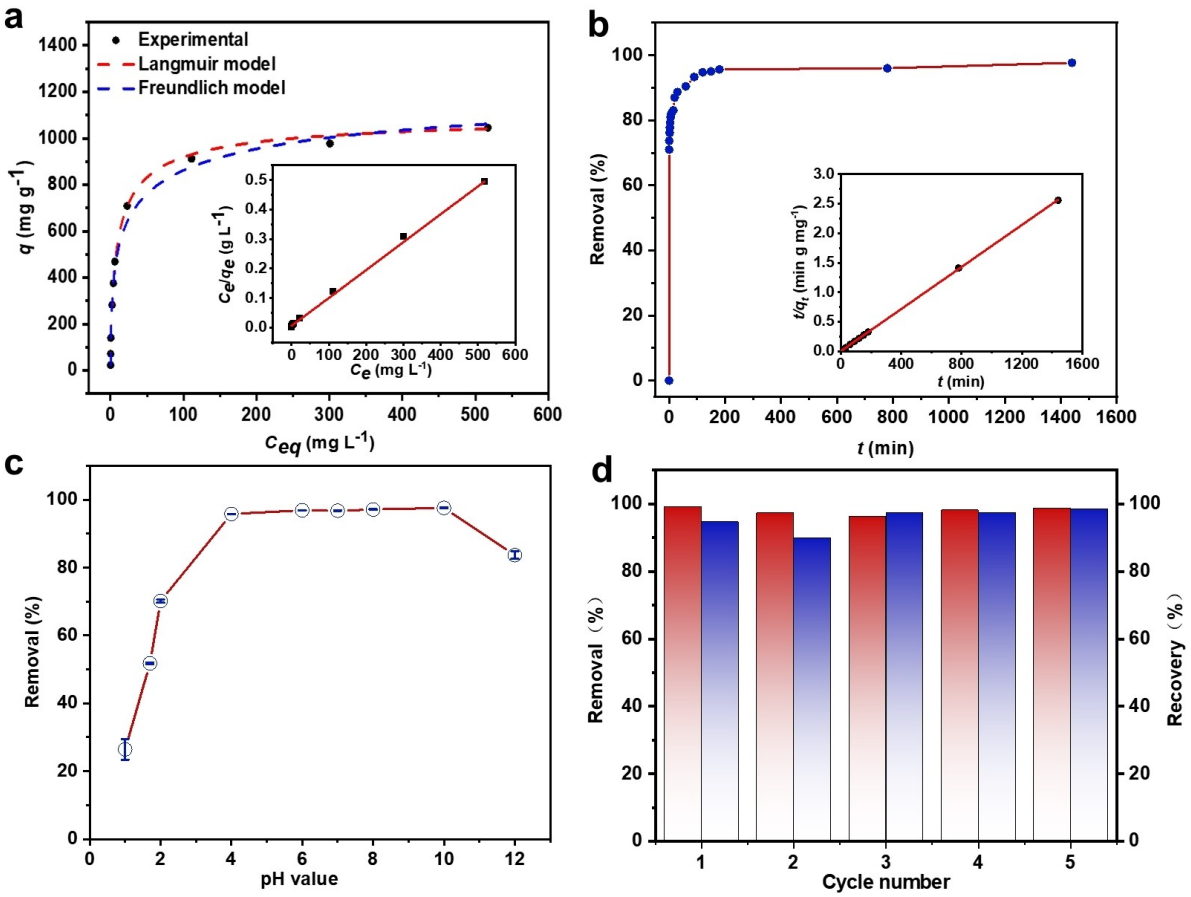

Figure 2. a) Sorption isotherm of CPN-3VIm-Cl for ReO_4^- uptake, inset shows the fitting curve based on the Langmuir model. b) Sorption kinetics of CPN-3VIm-Cl, inset shows the fitting curve based on the pseudo-second-order model. c) Effect of pH on the sorption properties of ReO_4^- by CPN-3VIm-Cl. d) Reversibility of CPN-3VIm-Cl, red columns show the uptake percentages for ReO_4^- and blue columns show the recovery percentages for ReO_4^-.

The adsorption kinetics of CPN-3VIm-Cl were investigated by collecting and isolating the material in solution at different times intervals, followed by analysis using Inductively Coupled Plasma Optical Emission Spectrometry (ICP-OES). As illustrated in Figure 2b, the removal rate surged to 74% within the initial minute, and further escalated to 87% within 20 minutes. This outcome signified a rapid adsorption kinetics, which holds significant implications for the treatment of industry wastewater. The pseudo-first-order model (Figure S9) and the pseudo-second-order model (inset in Figure 2b) were employed to fit the data. The results revealed that the adsorption kinetics of CPN-3VIm-Cl for ReO_4^- could be aptly described by the pseudo-second-order model, with a remarkably high correlation coefficient ($R^2 > 0.9999$, Table S2), indicating that the rate-determining step in the sorption process was predominantly chemical adsorption.

To delineate the applicable pH range of CPN-3VIm-Cl, a further exploration into the effect of pH on the material adsorption performance was conducted (ranging from 1 to 12). As shown in Figure 2c, the removal rate of ReO_4^- remained nearly invariant at around 100% within the pH range from 4 to 10. To unravel the underlying mechanism for the material's high tolerance across a wide pH range, Zeta Potential measurements were performed in solutions containing certain amounts of CPN-3VIm-Cl at different pH values. The results (Figure S10) indicated positive values throughout a broad pH range from 1 to 13, implying that CPN-3VIm-Cl retained positively charged over an extensive pH interval, endowing it with high adaptability to diverse wastewater systems.

Moreover, given its crucial importance in industrial applications, the recyclability of CPN-3VIm was evaluated. As shown in Figure 2d, even after four successive adsorption-desorption cycles, CPN-3VIm-Cl still attained an uptake percentage of 98.7% and a recovery percentage of 98.5% in the final cycle. With its broad pH adaptability and outstanding recyclability, CPN-3VIm-Cl manifested promising potential for application in the recovery and extraction of ReO_4^- from industrial wastewater.

Since industrial wastewater is replete with a multitude of competing anions, selectivity constitutes one of the pivotal factors for evaluating the performance of absorbent materials. In light of the actual industrial wastewater conditions prevalent in copper smelting plants, as well as diverse ion configurations and charge densities, NO_3^-, SO_4^{2-}, and AsO_4^{3-} were selected as competing ions to probe the selectivity of the material. As illustrated in Figure 3a, when the molar ratios of competing ions (NO_3^-, SO_4^{2-}, AsO_4^{3-}) to ReO_4^- were 10:1, the corresponding uptake efficiencies of ReO_4^- were 94.9%, 83.3%, and 89.1%,

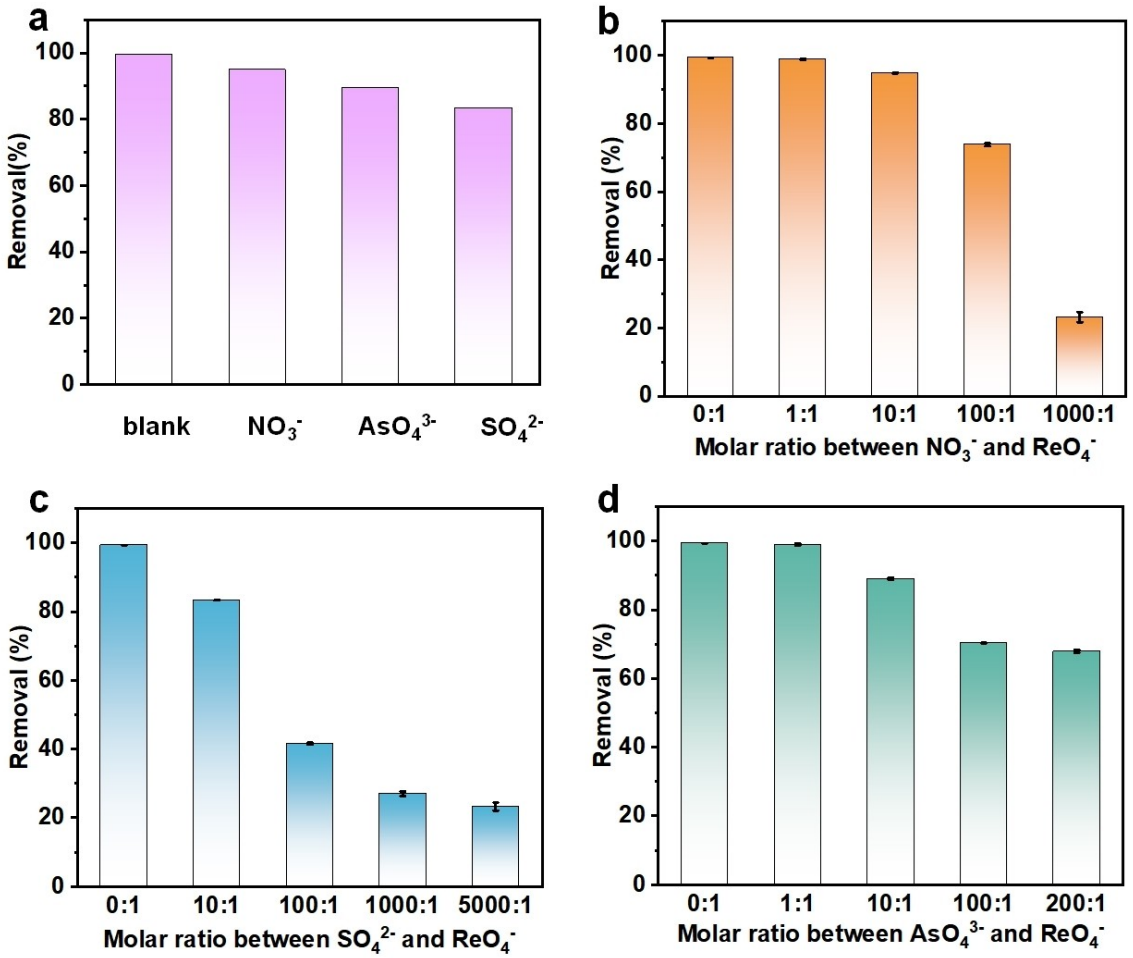

Figure 3. a) Effect of 10 eq competing anions (1.6×10^{-3} M) on the removal percentage of ReO_4^- (initial concentration of ReO_4^-: 1.6×10^{-4} M). b–d) Effect of competing NO_3^-, SO_4^{2-}, and AsO_4^{3-} anions, respectively, on the anion-exchange of ReO_4^- by CPN-3VIm-Cl.

respectively. Furthermore, comprehensive selectivity competition experiments were conducted with these three competing anions across a series of varying concentrations. The results demonstrated that when the molar ratios were extended to 100:1, the uptake efficiencies of ReO_4^- still persisted 73.9%, 41.5%, and 70.3%, respectively (Figure 3b–d). To simulate the conditions of actual smelting industrial wastewater more realistically, the molar ratios of competing ions (NO_3^-, SO_4^{2-}, AsO_4^{3-}) to ReO_4^- were adjusted to 1000:1, 5000:1 and 200:1, respectively. The outcome revealed that the uptake rates of ReO_4^- could still maintain as 23.2%, 23.3%, 68.0%, respectively. As reported in the literature, such selectivity was attributed to the stable face-to-face stacking structure between ReO_4^- and imidazolium cations.[4b] Overall, CPN-3VIm-Cl exhibited exemplary performance in terms of adsorption capacity, kinetics, recyclability and selectivity, thereby suggesting its promising potential application for ReO_4^- recovery in industrial wastewaters.

Sorption Mechanism

To gain a more profound understanding of the anion exchange process mechanism between CPN-3VIm-Cl and ReO_4^-, a series of comprehensive and in-depth analyses were conducted by employing techniques including Scanning electron microscopy-energy dispersive X-ray spectroscopy (SEM-EDS) mapping, FT-IR, Raman spectra, and X-ray photoelectron spectroscopy (XPS). Initially, SEM-EDS element analysis revealed that subsequent to the ion exchange process of CPN-3VIm in NaCl solution, there was a significant decline in the content of Br element, accompanied by a conspicuous increase in the Cl content (Figure 4a and Figure S12). Concurrently, based on the XPS survey spectrum of CPN-3VIm-Cl and the Cl 2p core-level spectrum, it was unequivocally demonstrated that the counterions of the cationic polymer have been fully replaced by chloride ions. After the capture of ReO_4^-, the chlorine element became scarcely detectable on the surface of the material, whereas the content of the rhenium element exhibited a remarkable augmentation. Moreover, as evidenced by the XPS survey spectra (Figure 4b), a clear disappearance of the Cl 2p peak (Figure 4f) and the emergence of the Re 4f peak (Figure

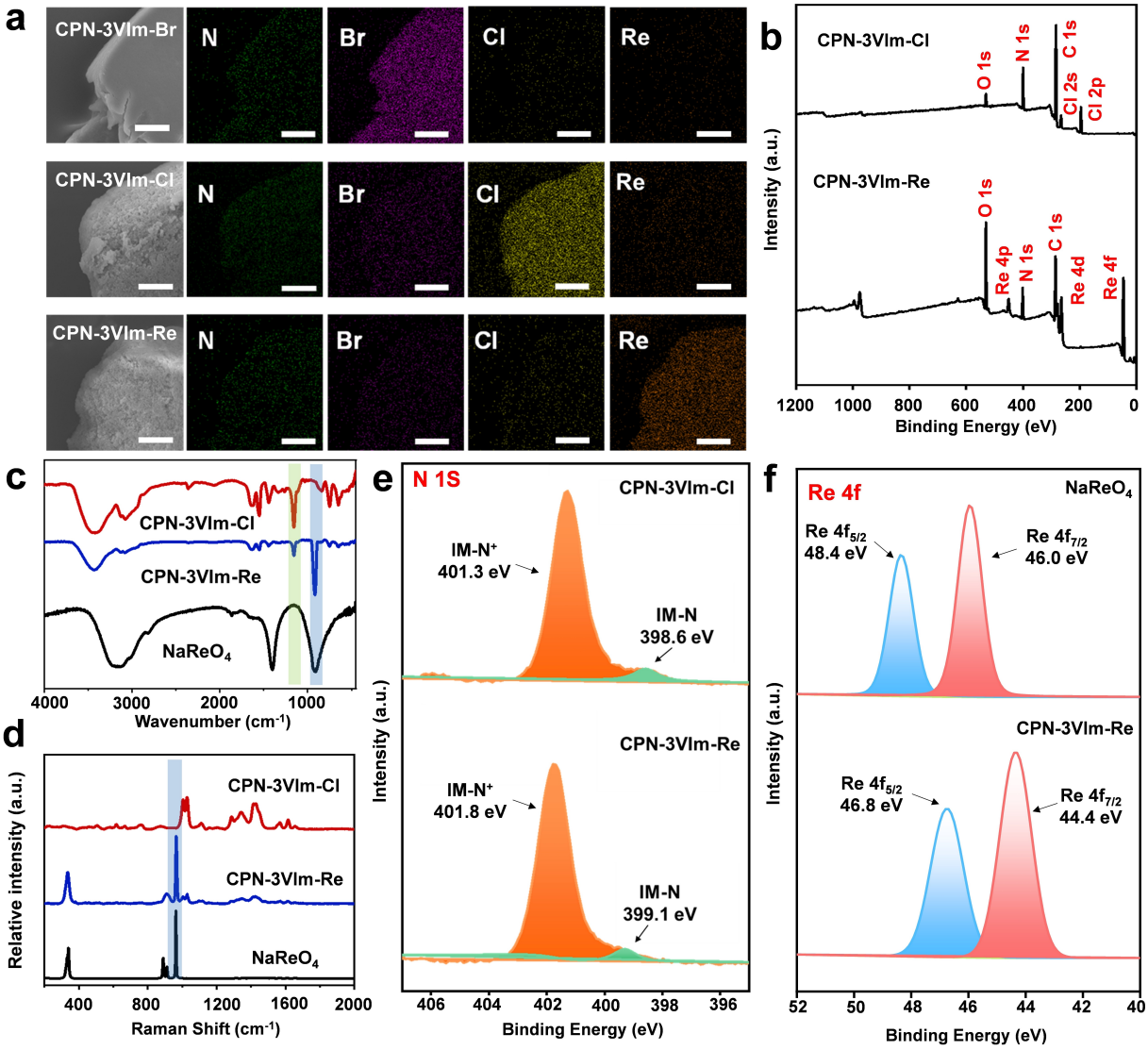

Figure 4. a) SEM-EDS mapping of CPN-3VIm-Br, CPN-3VIm-Cl, and CPN-3VIm-Re, scale bar = 700 nm. b) XPS survey spectra of CPN-3VIm-Cl and CPN-3VIm-Re. c) FT-IR spectra of CPN-3VIm before and after anion-exchange with ReO_4^- and $NaReO_4$. Characteristics peaks occurring at 1074 cm^{-1} (green band) and 902 cm^{-1} (blue band) corresponded to the quaternary imidazolium species and ReO_4^-, respectively. d) Raman spectra of CPN-3VIm before and after anion-exchange with ReO_4^- and $NaReO_4$. Characteristics peaks occurring at 965 cm^{-1} (blue band). e) N 1s core-level spectra of CPN-3VIm-Cl and CPN-3VIm-Re. f) XPS analysis of Re 4f from CPN-3VIm-Re and $NaReO_4$.

S11) were discernible upon comparing the XPS spectrum of CPN-3VIm-Cl and CPN-3VIm-Re. These findings strongly suggested that an almost complete ion exchange process had occurred between Cl^- and ReO_4^-.

In addition, a meticulous analysis of the high-resolution XPS spectrum of CPN-3VIm-Re was conducted to elucidate the electronic states of Re 4f and N 1s (Figure 4e and 4f). The examination of the N 1s high-resolution spectrum of CPN-3VIm-Re revealed two distinct peaks. The sharp peak corresponding to a relatively high binding energy was ascribed to the imidazolium nitrogen cation (IM-N^+), whereas the broader peak at a lower binding energy was attributed to the non-ionic N atoms on the imidazole ring (IM–N). For the Re 4f spectrum, it comprised two peaks: Re $4f_{5/2}$ (46.8 eV) and Re $4f_{7/2}$ (44.4 eV), indicating that the oxidation state of Re on the polymer surface was Re(VII). Furthermore, by correlating the characteristic adsorption peaks of ReO_4^- appear at 912 cm^{-1} in the FT-IR spectrum and 965 cm^{-1} in the Raman spectrum of CPN-3VIm-Re (Figures 4c and 4d), the presence of adsorbed ReO_4^- was firmly corroborated.[4b]

Moreover, when compared with the high-resolution XPS spectrum of CPN-3VIm-Cl prior to adsorption and using $NaReO_4$ as a reference, the N 1s and Re 4f peaks of CPN-3VIm-Re exhibited binding energy differences of 0.5 eV and 1.6 eV, respectively (Figure 4e and 4f). This outcome signified a robust interaction between the imidazolium cation and ReO_4^-.[22] Additionally, both the FT-IR and Raman spectra (Figure 4c and 4d) revealed that the original characteristic adsorption peaks of the material remained well-preserved after the ion exchange process, implying that the structural skeleton of CPN-3VIm-Cl

was preserved after the adsorption of ReO_4^-. This further substantiated the fact that the adsorption of ReO_4^- by the material essentially involved ion exchange between Cl^- and ReO_4^-, without altering the structural skeleton itself.

Conclusions

In summary, this study presents a comprehensive exploration of the perrhenate adsorption capabilities exhibited by cationic polymeric nanotrap, CPN-3VIm-Cl, with a particular emphasis on its prospective applications in industrial wastewater treatment. Remarkably, the maximum adsorption capacity of this polymer could reach up to 1220 $mg \cdot g^{-1}$, facilitating an extremely efficient adsorption process that could reduce the perrhenate concentration down to a mere 39.9 ppb. Even after enduring five consecutive cycles of adsorption-desorption procedures, the removal and recovery rates remained remarkably robust, registering as 98.7% and 98.5%, respectively. This not only attests to the material's excellent adsorption efficiency but also highlights its reusability potential. Moreover, across a wide pH range from 1 to 12, the surface of CPN-3VIm-Cl consistently maintained positively charged, a characteristic that endows it with exceptional adaptability in diverse aqueous environments. Notably, within the pH range of 4-10, the removal rate was impressively sustained at nearly 100%, signifying its stability and effectiveness under typical industrial wastewater pH conditions. Furthermore, the material's structural integrity was found to be highly resilient, as it could preserve its stable structure even after being soaked in strong acid solutions overnight. These outstanding attributes unequivocally establish that the cationic polymer CPN-3VIm-Cl exhibited exceptional adsorption performance for ReO_4^- and remarkable structural stability. Such performance positions it as a highly promising candidate for application in complex and diverse rhenium-containing wastewater processes, thereby providing valuable guidance for industrial rhenium extraction from wastewater.

Acknowledgements

The authors acknowledge the financial support received from the National Natural Science Foundation of China (52304421, 22101302), Natural Science Foundation of Hunan Province (2022JJ20053, 2022JJ10071, 2023JJ40230), China Scholarship Council (CSC) (201706370186). Partial support from the Robert A. Welch Foundation (B-0027) is also acknowledged (S.M.) and Energy Innovation Research Chair at Princess Nourah bint Abdulrahman University (Grant no.1) (T.A.) (T.A.).

Conflict of Interests

The authors declare no conflict of interest.

Data Availability Statement

The data that support the findings of this study are available from the corresponding author upon reasonable request.

Keywords: Perrhenate anion · Cationic polymeric nanotraps · Imidazolium · Ion exchange

[1] a) *Mineral Commodity Summaries*, Reston, VA, **2024**, p. 212; b) H. S. Kim, J. S. Park, S. Y. Seo, T. Tran, M. J. Kim, *Hydrometallurgy* **2015**, *156*, 158–164.
[2] a) H. Hu, L. Sun, B. Jiang, H. Wu, Q. Huang, X. Chen, *Miner. Eng.* **2018**, *124*, 123–136; b) C. D. Anderson, P. R. Taylor, C. G. Anderson, *Miner. Metall. Proc.* **2013**, *30*, 59–73; c) H. Hu, B. Jiang, J. Zhang, X. Chen, *RSC Adv.* **2015**, *5*, 104769–104778.
[3] N. Nebeker, J. B. Hiskey, *Hydrometallurgy* **2012**, *125–126*, 64–68.
[4] a) X. Li, L. Chai, J. Ren, L. Jin, H. Wang, Y. Li, S. Ma, *Polym. Chem.* **2022**, *13*, 156–160; b) X. Li, Y. Li, H. Wang, Z. Niu, Y. He, L. Jin, M. Wu, H. Wang, L. Chai, A. M. Al-Enizi, A. Nafady, S. F. Shaikh, S. Ma, *Small* **2021**, *17*, 2007994.
[5] X. Zhang, M. Hao, X. Yang, Z. Chen, S. Wang, H. Yang, X. Wang, *Natl. Sci. Open* **2024**, *4*, 20240007 .
[6] a) H. Dai, X. Yuan, L. Jiang, H. Wang, J. Zhang, J. Zhang, T. Xiong, *Coord. Chem. Rev.* **2021**, *441*, 213985; b) D. Sheng, L. Zhu, X. Dai, C. Xu, P. Li, C. Pearce, C. Xiao, J. Chen, R. Zhou, T. Duan, O. K. Farha, Z. Chai, S. Wang, *Angew. Chem. Int. Ed.* **2019**, *58*, 4968–4972; c) D. P. Sheng, L. Zhu, C. Xu, C. L. Xiao, Y. L. Wang, Y. X. Wang, L. H. Chen, J. Diwu, J. Chen, Z. F. Chai, T. E. Albrecht-Schmitt, S. A. Wang, *Environ. Sci. Technol.* **2017**, *51*, 3471–3479.
[7] a) Z. Dong, N. Zhang, M. Zhang, M. Yang, Q. Bao, L. Zhao, *New J. Chem.* **2023**, *47*, 8809–8819; b) S. Lin, J. Mao, J. Xiong, Y. Tong, X. Lu, T. Zhou, X. Wu, *Chemosphere* **2023**, *345*, 140485–140485; c) D. Li, J. C. Seaman, S. E. Hunyadi Murph, D. I. Kaplan, K. Taylor-Pashow, R. Feng, H. Chang, M. Tandukar, *J. Hazard. Mater.* **2019**, *374*, 177–185.
[8] a) A. Muhammad, Q. Yang, A. Kanwal, J. Zhao, M. Nawaz, H. Ren, P. Yang, *Sci. China Technol. Sci.* **2023**, *67*, 1417–1430; b) L. Peng, M. Zhang, Z. Dong, J. Du, W. Li, L. Zhao, *J. Mol. Liq.* **2024**, *394*, 123709; c) N. Wang, M. Zhang, Z. Dong, L. Peng, M. Zhai, L. Zhao, *Radiat. Phys. Chem.* **2023**, *209*, 110950; d) C. P. Li, H. Zhou, J. Chen, J. J. Wang, M. Du, W. Zhou, *ACS Appl. Mater. Interfaces* **2020**, *12*, 15246–15254; e) L. Zhu, C. L. Xiao, X. Dai, J. Li, D. X. Gui, D. P. Sheng, L. H. Chen, R. H. Zhou, Z. F. Chai, T. E. Albrecht-Schmitt, S. Wang, *Environ. Sci. Technol. Lett.* **2017**, *4*, 316–322.
[9] a) J.-X. Qi, C.-R. Zhang, X.-J. Chen, S.-M. Yi, C.-P. Niu, J.-L. Liu, L. Zhang, R.-P. Liang, J.-D. Qiu, *Anal. Chem.* **2022**, *94*, 10850–10856; b) S.-M. Yi, C.-R. Zhang, X. Liu, W. Jiang, R.-P. Liang, J.-D. Qiu, *Mater. Chem. Phys.* **2023**, *306*, 128032; c) J. Li, X. Dai, L. Zhu, C. Xu, D. Zhang, M. A. Silver, P. Li, L. H. Chen, Y. Z. Li, D. W. Zuo, H. Zhang, C. L. Xiao, J. Chen, J. Diwu, O. K. Farha, T. E. Albrecht-Schmitt, Z. F. Chai, S. A. Wang, *Nat. Commun.* **2018**, *9*, 3007; d) Q. Sun, L. Zhu, B. Aguila, P. K. Thallapally, C. Xu, J. Chen, S. Wang, D. Rogers, S. Ma, *Nat. Commun.* **2019**, *10*, 1646; e) J. Li, B. Li, N. Shen, L. Chen, Q. Guo, L. Chen, L. He, X. Dai, Z. Chai, S. Wang, *ACS Cent. Sci.* **2021**, *7*, 1441–1450.
[10] a) D. S. Morris, K. van Rees, M. Curcio, M. Cokoja, F. E. Kuehn, F. Duarte, J. B. Love, *Catal. Sci. Technol.* **2017**, *7*, 5644–5649; b) W. Xu, X. Wang, Y. Li, W.-R. Cui, *J. Hazard. Mater.* **2023**, *455*, 131549.
[11] a) R. Luo, X. Liu, M. Chen, B. Liu, Y. Fang, *ChemSusChem* **2020**, 3945–3966; b) B. Wang, J. Li, H. Huang, B. Liang, Y. Zhang, L. Chen, K. Tan, Z. Chai, S. Wang, J. T. Wright, R. W. Meulenberg, S. Ma, *ACS Cent. Sci.* **2024**, *10*, 426–438.
[12] a) M. Ding, L. Chen, Y. Xu, B. Chen, J. Ding, R. Wu, C. Huang, Y. He, Y. Jin, C. Xia, *Chem. Eng. J.* **2020**, *380*, 122581; b) B. Y. Li, Y. M. Zhang, D. X. Ma, Z. Y. Xing, T. L. Ma, Z. Shi, X. L. Ji, S. Q. Ma, *Chem. Sci.* **2016**, *7*, 2138–2144.
[13] a) A. D. Pant, R. Ruhela, C. Limje, M. Vartak, A. K. Yadav, A. S. Kumar, A. K. Singh, S. N. Jha, D. Bhattacharya, V. Kain, B. S. Tomar, *Ind. Eng. Chem. Res.* **2021**, *60*, 551–557; b) H.-R. Li, S. Wu, X. Jing, Z. Di, K. Liu, L. Wang, C.-P. Li, Z. Liu, M. Du, *Sci. China Chem.* **2024**, *67*, 2958–2967.
[14] X. Li, L. Jin, L. Huang, X. Ge, H. Deng, H. Wang, Y. Li, L. Chai, S. Ma, *J. Environ. Chem. Eng.* **2021**, *9*, 106357.
[15] S. Yang, J. Yin, Q. Li, C. Wang, D. Hua, N. Wu, *J. Hazard. Mater.* **2022**, *429*, 128315.

[16] a) H. Fan, J. Wang, Z. Tao, J. Huang, P. Rao, T. Kurokawa, J. P. Gong, *Nat. Commun.* **2019**, *10*, 5127; b) D. Banerjee, D. Kim, M. J. Schweiger, A. A. Kruger, P. K. Thallapally, *Chem. Soc. Rev.* **2016**, *45*, 2724–2739.
[17] J. R. Keith, N. J. Rebello, B. J. Cowen, V. Ganesan, *ACS Macro Lett.* **2019**, *8*, 387–392.
[18] a) X. Suo, X. Cui, L. Yang, N. Xu, Y. Huang, Y. He, S. Dai, H. Xing, *Adv.Mater.* **2020**, *32*, 1907601; b) Q.-H. Hu, W. Jiang, R.-P. Liang, S. Lin, J.-D. Qiu, *Chem. Eng. J.* **2021**, *419*, 129546; c) Y. Xie, J. Liang, Y. Fu, M. Huang, X. Xu, H. Wang, S. Tu, J. Li, *J. Mater. Chem. A* **2018**, *6*, 6660–6666.
[19] D. Han, X. Li, J. Peng, L. Xu, J. Li, H. Li, M. Zhai, *RSC Adv.* **2016**, *6*, 69052–69059.
[20] a) W. Wang, M. Xu, P. Liu, H. Yu, L. Zhang, D. Hua, *Sep. Purif. Technol.* **2024**, *344*, 127294; b) J. Li, L. Chen, N. Shen, R. Xie, M. V. Sheridan, X. Chen, D. Sheng, D. Zhang, Z. Chai, S. Wang, *Sci. Chi. Chem.* **2021**, *64*, 1251–1260.
[21] a) Y. Li, L. Wang, Y. Cao, S. Xu, P. He, H. Li, H. Liu, *RSC Adv.* **2021**, *11*, 14193–14202; b) Z. Lou, T. Li, X. Tao, X. Zhou, W. Zhao, J. Cui, X. Feng, H. Yu, Y. Wang, W. Shan, Y. Xiong, *J. Membr. Sci.* **2024**, *692*, 122285.
[22] Z. W. Liu, B. H. Han, *Environ. Sci. Technol.* **2020**, *54*, 216–224.

Manuscript received: October 15, 2024
Revised manuscript received: January 5, 2025
Accepted manuscript online: January 20, 2025
Version of record online: ■■, ■■

RESEARCH ARTICLE

Herein, we report the efficient capture behavior for perrhenate by the cationic polymeric nanotrap CPN-3VIm-Cl. The material shows a maximum capacity up to 1220 mg·g^{-1} for ReO_4^- uptake, with an adsorption rate exceeding 99% even in a low-concentration ReO_4^- solution of 8.5 ppm. Furthermore, CPN-3VIm-Cl achieves nearly 100% extraction efficiency for ReO_4^- in a wide pH range from 4 to 10.

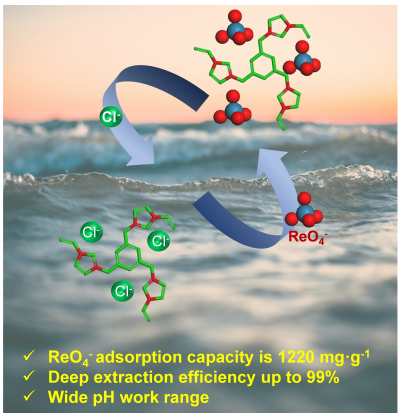

X. Li, W. Liu, Prof. H. Wang, Y. He, Prof. W. Liu, H. Li, L. Jin, C. Su, Prof. Y. Li, T. AlShahrani, Prof. S. Ma**